An efficient deep learning approach to identify dynamics in *in vitro* neural networks

Vito Paolo Pastore[1,2], Giulia Parodi[2], Martina Brofiga[2,3], Paolo Massobrio[2,4], Michela Chiappalone[2], *Member IEEE*, Francesca Odone[1,2] and Sergio Martinoia[2,5], *Member IEEE*

***Abstract*— Understanding and discriminating the spatiotemporal patterns of activity generated by *in vitro* and *in vivo* neuronal networks is a fundamental task in neuroscience and neuroengineering. The state-of-the-art algorithms to describe the neuronal activity mostly rely on global and local well-established spike and burst-related parameters. However, they are not able to capture slight differences in the activity patterns. In this work, we introduce a deep-learning-based algorithm to automatically infer the dynamics exhibited by different neuronal populations. Specifically, we demonstrate that our algorithm is able to discriminate with high accuracy the dynamics of five different populations of *in vitro* human-derived neural networks with an increasing inhibitory to excitatory neurons ratio.**

I. INTRODUCTION

Despite significant progress in electrophysiology and imaging techniques *in vivo*, understanding how information is transmitted and processed in the human brain is still a utopia [1]. In this perspective, over the years, simplified experimental models have been proposed, such as primary neuronal cultures *in vitro*. More recently, thanks to the use of human-induced pluripotent stem cells (h-iPSCs), *in vitro* neuronal networks reproducibly and reliably approach the activity and processes of the human brain [2], [3]. By combining these *in vitro* systems with Micro-Electrode Arrays (MEAs) technology, new horizons are opening up in the fields of neuroscience and precision medicine [4]. Despite the reduction in complexity of the system (from *in vivo* to *in vitro*) and the large body of literature available on the analysis of MEA-based recordings [5]–[7], the electrophysiological patterns of activity from *in vitro* networks are still extremely intricate. For this reason, extrapolating global and local dynamic parameters [8] to analyze and classify them, is a long process that can be onerous and challenging. To overcome these difficulties and limitations, in this study, we introduce a deep-learning-based algorithm to automatically infer the dynamics of *in-vitro* neural networks coupled to MEAs. In recent years, deep-learning (DL) approaches have gained particular popularity for the analysis of physiological signals thanks to their potential in simplifying complex classification tasks [9]. DL has been mainly exploited for the evaluation of electrocardiogram (ECG) signals for the classification of heart diseases by exploiting features extraction from ECG [10] or by processing the ECG as images [11]. Another widely used application of DL-based algorithms is the classification of electroencephalograms (EEG) features to detect sleep phases [12], epileptic disorders [13] or to diagnose Parkinsons disease [14]. As regards Local Field Potentials (LFPs), their analysis with a DL-based algorithm has been exploited to localize the subthalamic nucleus for the parameters tuning of deep brain stimulation, in treating Parkinsons disease [15]. At the spike level, the DL-based techniques are mostly focused on the localization, classification, and morphological characterization of single neurons [16], [17]. In our work, we are making a step forward by exploiting DL to identify the different patterns of activity emerging in neuronal networks. Interestingly, our method overcomes the concept of feature extraction, directly processing the neuronal signals as images of the spiking activity. As experimental model, we adopted h-iPSCs-derived networks composed of glutamatergic and GABAergic neurons obtained from healthy subjects in which the ratio between excitation and inhibition (E/I ratio) has been varied. Our hypothesis was that the recorded electrophysiological activity would have been influenced by the E/I ratio and, as a consequence, these imbalances would have been reflected by the exhibited neuronal dynamics [18], [19]. Hence, the main aim of our work is to provide an efficient method for correctly classifying different activity patterns and thus distinguishing the nature of the neuronal population generating them, without performing any detection of bursts or network bursts. We conclude that thanks to this method, it is not necessary to carry out in-depth extrapolations of parameters, leading to rapid dynamics identification.

[1]Machine Learning Genoa Center (MaLGa), Department of Informatics, Bioengineering, Robotics and Systems Engineering, University of Genova, Genova, Italy {Vito.Paolo.Pastore,Francesca.Odone}@unige.it

[2] Department of Bioengineering, Robotics and System Engineering, Genova, Italy Giulia.Parodi@edu.unige.it, Martina.Brofiga@dibris.unige.it {Paolo.Massobrio,Michela.Chiappalone, Sergio.Martinoia}@unige.it

[3]ScreenNeuroPharm s.r.l, Sanremo, Italy

[4]INFN, National Institute for Nuclear Physics, Genova, Italy

[5]CNRInstitute of Biophysics, Genova, Italy

II. METHODS

A. Data acquisition

H-iPSCs-derived neuronal networks were obtained with the overexpression of Neurogenin 2 (Ngn-2) and of Achaete-Scute homolog 1 (Ascl1), induced by the introduction of doxycycline and forskolin in the culture medium [20]. The neuronal networks were composed of glutamatergic and GABAergic neurons mixed in appropriate proportion to obtain 5 different configurations described in II-B. The neurons were co-plated with rat astrocytes (30%) to ensure proper sustain and to favor neuronal growth. Cells were plated on

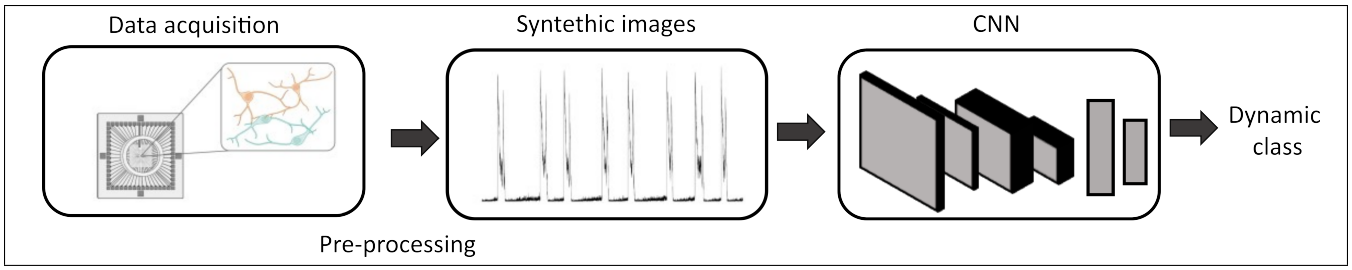

Figure 1. Schematic representation of the proposed pipeline.

MEAs (1200 cells/mm^2) pre-coated with human-laminin (20 ţg/ml, BioLamina) and poly-L-ornithine (50 ţg/ml, Sigma-Aldrich) overnight. The neuronal networks were cultured in Neurobasal medium (Thermo Fisher Scientific) supplemented with B27 (2%, Thermo Fisher Scientific), penicillin/streptomycin (1%, Sigma-Aldrich), stable L-Glutamine (1% GlutaMAX 100x, GIBCO Invitrogen), human Brain-Derived Neurotrophic Factor (BDNF, 10 ng/ml, Sigma-Aldrich), human Neurotrophin-3 (NT-3, 10 ng/ml, Sigma-Aldrich), doxycycline (4 ţg/ml, Sigma-Aldrich), forskolin (4 ţg/ml, Sigma-Aldrich) and Fetal Bovine Serum (FBS, 2% Thermo Fisher Scientific). At day *in vitro* (DIV) 70, we recorded the electrophysiological basal activity of the neuronal networks for 15 minutes at 10 kHz in stable condition (37řC/ 5%CO_2), by using the MEA2100 recording system (Multi Channel Systems-MCS, Reutlingen, Germany).

B. Dataset description and pre-processing analysis

We recorded 15 minutes of electrophysiological spontaneous activity at DIV 70 of different *in-vitro* neural networks with the following inhibitory to excitatory neurons ratio (*E/I ratio*): (i) 100E0I; (ii) 75E25I; (iii) 50E50I; (iv) 25E75I; (v) 0E100I. We acquired 7 devices for the classes 75E25I and 25E75I and 6 devices for each of the remaining ones. To identify the spike activity, we performed the precision time spike detection algorithm [21] on the acquired recordings. Eventually, raster plots and cumulative spike trains were computed. We binned the cumulative spike trains with a 10 ms time window. We computed the total number of spikes detected in each bin for the entire set of channels (60) and we built the corresponding histograms.

C. Histograms and raster plots as images

The main idea of our algorithm was to treat the computed raster plots and cumulative spikes time histograms as synthetic images. In this way, it was possible to exploit image processing DL-based algorithms for the solution of the task at hand. However, DL algorithms are notoriously data-hungry. Thus, we further split the obtained raster plots and histograms with different time bins to increase the number of available images. We considered four different candidates' time bins: (i) 120 s; (ii) 60 s; (iii) 30 s and (iv) 10 s. Moreover, we considered a stride of 5 s between consecutive bins to avoid the risk of losing informative dynamic events in the pre-processing. See Fig. 2 for an example of the representative cumulative spike time histograms images with a time bin of 120 s. Thus, the input dataset for our deep learning models is $d = x, y$, where x represents the images corresponding to either the cumulative spikes time histograms or the raster plots, and $y \in [0, 4]$ representing the specific class of neural matrices among the available five described in Sect. II-B.

D. Proposed pipeline

Fig. 1 shows a schematic overview of the designed pipeline. The first step is the pre-processing of the acquired data to be used as input for a deep neural network. Spike detection was performed on the raw data, to build raster plots and cumulative spike time histograms (see Sect. II-B). The two dynamic information were further processed to obtain synthetic images as explained in Sect. II-C. The synthetic images were then used as input to a deep neural network. We exploited a transfer-learning framework to compensate for the low amount of available data. Thus, we adopted a deep neural network pre-trained on a large-scale natural image dataset (i.e., ImageNet) as a features extractor [22], adding a shallow classifier with two fully connected layers, one with 64 neurons and the output one with a number of neurons equal to the number of dynamic classes (five for the dataset used in this work, see section II-B).

III. Experiments

A. Experiment details

We performed a leave-one-out cross-validation approach in our experiments, as we have a total of 32 devices available. Thus, we performed 32 training processes, each time using one of the available devices as a test, and the remaining 31 to train our deep neural networks. We further perform a cross-validation procedure to tune the training hyperparameters. We trained our neural networks for 25 epochs, with an Adam optimizer (learning rate equal to 0.0005), a batch size of 75 and an exponential learning rate scheduler.

B. Results

Our first experiment consisted of evaluating the performances of our pipeline with respect to the different synthetic input images (cumulative spike train histograms or raster plots) and the time bin used for generating them (10, 30, 60, or 120 seconds). We used an EfficientNetB0 ImageNet pre-trained neural network as a features extractor for this experiment.

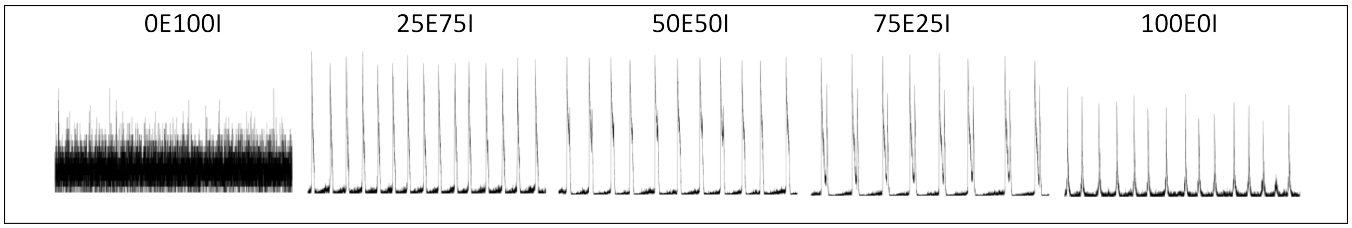

Figure 2. Synthetic images of representative cumulative spike time histograms for each class of culture included in this work. Each image corresponds to a time bin of 120 seconds.

TABLE I

ACCURACY AND STANDARD DEVIATION CORRESPONDING TO THE LEAVE-ONE-OUT CROSS-VALIDATION APPROACH PERFORMED WITH EFFICIENTNETB0 ON THE 32 AVAILABLE DEVICES.

Input image	Window	Acc s_image	Acc device
Histogram	120	$\mathbf{0.747 \pm 0.353}$	$\mathbf{0.813}$
Histogram	60	0.670 ± 0.398	0.688
Histogram	30	0.665 ± 0.378	0.656
Histogram	10	0.659 ± 0.358	0.719
Raster Plot	120	0.580 ± 0.400	0.563
Raster Plot	60	0.567 ± 0.415	0.625
Raster Plot	30	0.659 ± 0.403	0.656
Raster Plot	10	0.652 ± 0.398	0.688

Table I shows the obtained results in terms of average test accuracy among the 32 leave-one-out folds. A time bin of 120 seconds with cumulative spike time histograms leads to the best test accuracy, equal to 0.747 considering the single synthetic images prediction (s_image in Table I), and 0.813 on the whole devices (26 devices correctly classified over a total of 32). Fig. 2a shows the corresponding confusion matrix. As we can see, the misclassified devices belong to the 50E50I and the 75E25I classes. Our hypothesis is that the dynamics of these classes can be fuzzy due to the unpredictable reshaping of the plated neurons with the emergence of common temporal patterns. According to this, we performed another experiment, training an EfficientNetB0 with the best-performing parameters (time bin of 120 seconds with cumulative spike time histograms), but grouping all the classes composed by both excitatory and inhibitory neurons (i.e., 25E75I, 50E50I, 75E25I) in a superclass that we called *heterogeneous configuration*. Fig. 2b shows the confusion matrix obtained on the 32 leave-one-out folds. The algorithm made only one mistake (with one mixed inhibition classified as 100E0I), corresponding to an average test accuracy of 0.957 ± 0.175 on the single synthetic images and 0.969 on the whole devices. We later evaluated the performances of our algorithm with respect to the neural network architecture used as a feature extractor, on the original multi-class classification problem with 5 classes. We compared six different neural network architectures, with an increasing depth and number of parameters. For this set of experiments, we fixed the time bin and the input image to 120 seconds and cumulative spike train histograms, respectively, as they led to the highest test accuracy for EfficientNetB0. Table II reports the obtained results, in terms of average test accuracy computed for the 32 leave-one-out folds. The EfficientNetB0 model outperformed the benchmark neural networks. Excluding a drop in accuracy for the smallest network (MobileNetv2), all the investigated models showed comparable results in terms of test accuracy, proving the robustness of the proposed algorithm. Our pipeline is computationally very efficient, as the ImageNet pre-trained deep neural networks are used as feature extractors, and only a shallow classifier with two layers is trained. The average total training time for the best performing configuration (5024 synthetic images in training) is ≈ 55 seconds (40 seconds needed to extract features and 15 seconds to train the classifier). The inference rate is ≈ 63 Hz. We performed our experiments on a laptop with a core i7 2.5 GhZ processor, 16 GB of RAM, and an Nvidia RTX 3060 GPU with 6 GB of RAM.

TABLE II

ACCURACY AND STANDARD DEVIATION CORRESPONDING TO THE LEAVE-ONE-OUT CROSS-VALIDATION APPROACH AT THE VARYING OF THE NETWORK ARCHITECTURE ON THE 32 AVAILABLE DEVICES. RESULTS ARE REPORTED ONLY FOR THE BEST TIME BIN (I.E., 120 S).

Architecture	Parameters (M)	Acc sw	Acc device
EfficientNetB0	5.3	$\mathbf{0.747 \pm 0.353}$	$\mathbf{0.813}$
DenseNet121	8.1	0.671 ± 0.377	0.719
DenseNet201	20.2	0.721 ± 0.391	0.750
EfficientNetB1	7.9	0.716 ± 0.396	0.719
Xception	22.9	0.684 ± 0.389	0.750
MobileNetv2	3.5	0.618 ± 0.384	0.625

IV. CONCLUSIONS

In this work, we introduced a deep learning-based pipeline to automatically infer the dynamic of *in vitro* neural networks. The main idea was to exploit cumulative spike time histograms to obtain synthetic images. These images were fed to a deep neural network to obtain dynamic class predictions. We tested our pipeline on a challenging dataset, represented by five different *in vitro* neural networks with increasing percentages of inhibitory neurons (from 0 to 100 % with a step of 25%). We obtained the best performances using an ImageNet pre-trained EfficientNetB0 and a time bin of 120 seconds to create our input images. With this configuration, we were able to correctly classify 26 devices over a total of 32 with the proposed approach. Finally, our method is very efficient, requiring less than one minute for training and being able to predict the dynamic of 63 synthetic images in one second (i.e., 2.5 seconds on average to infer the class of a device). Thus, it is compatible with an online real-time analysis.

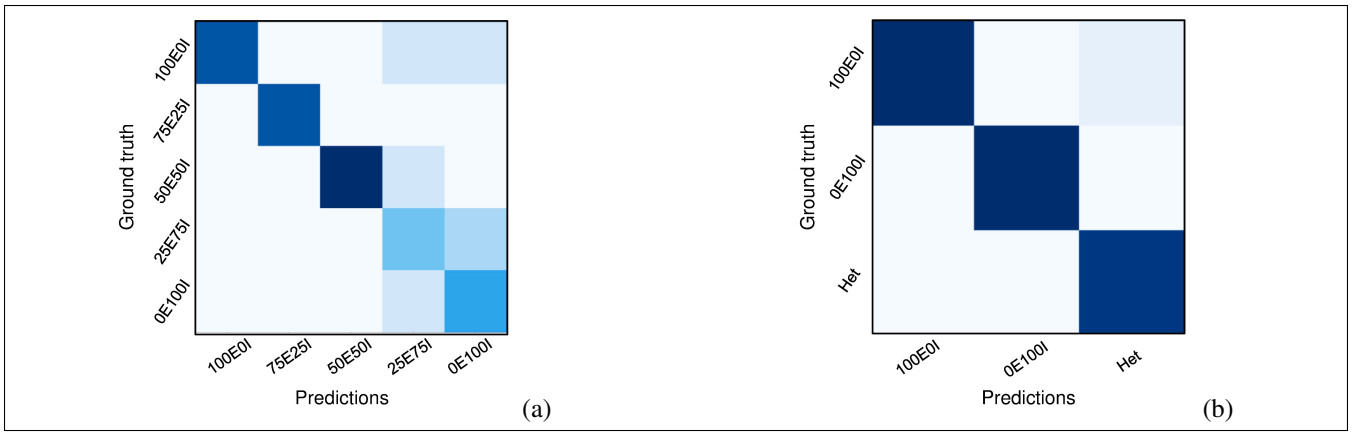

Figure 3. Confusion matrices correspondent to our best performing configuration (EfficientNetB0, Cumulative Spike Time Histogram, and time bin of 120 seconds). (a) Original 5 classes; (b) reduced labels corresponding to the fusion of heterogeneous inhibition classes.

ACKNOWLEDGMENT

VPP has been supported by funding from the European Union FSE REACT-EU-PON Ricerca e Innovazione, DM 1062/2021. Contract # 11-G-14987-1.

REFERENCES

[1] Martina Brofiga, Marietta Pisano, Roberto Raiteri, and Paolo Massobrio, "On the road to the brain-on-a-chip: a review on strategies, methods, and applications," *Journal of Neural Engineering*, vol. 18, no. 4, pp. 041005, 2021.

[2] Britt Mossink, Anouk HA Verboven, Eline JH van Hugte, Teun M Klein Gunnewiek, Giulia Parodi, Katrin Linda, Chantal Schoenmaker, Tjitske Kleefstra, Tamas Kozicz, Hans van Bokhoven, et al., "Human neuronal networks on micro-electrode arrays are a highly robust tool to study disease-specific genotype-phenotype correlations in vitro," *Stem cell reports*, vol. 16, no. 9, pp. 2182–2196, 2021.

[3] Kazuyuki Fukushima, Yuji Miura, Kohei Sawada, Kazuto Yamazaki, and Masashi Ito, "Establishment of a human neuronal network assessment system by using a human neuron/astrocyte co-culture derived from fetal neural stem/progenitor cells," *Journal of biomolecular screening*, vol. 21, no. 1, pp. 54–64, 2016.

[4] Martina Brofiga and Paolo Massobrio, "Brain-on-a-chip: Dream or reality?," *Frontiers in Neuroscience*, vol. 16, 2022.

[5] Hiroyuki Kamioka, Eisaku Maeda, Yasuhiko Jimbo, Hugh PC Robinson, and Akio Kawana, "Spontaneous periodic synchronized bursting during formation of mature patterns of connections in cortical cultures," *Neuroscience letters*, vol. 206, no. 2-3, pp. 109–112, 1996.

[6] Vito Paolo Pastore, Daniele Poli, Aleksandar Godjoski, Sergio Martinoia, and Paolo Massobrio, "Toolconnect: a functional connectivity toolbox for in vitro networks," *Frontiers in neuroinformatics*, vol. 10, pp. 13, 2016.

[7] Vito Paolo Pastore, Paolo Massobrio, Aleksandar Godjoski, and Sergio Martinoia, "Identification of excitatory-inhibitory links and network topology in large-scale neuronal assemblies from multi-electrode recordings," *PLoS computational biology*, vol. 14, no. 8, pp. e1006381, 2018.

[8] Vito Paolo Pastore, Aleksandar Godjoski, Sergio Martinoia, and Paolo Massobrio, "S pi c o d yn: A toolbox for the analysis of neuronal network dynamics and connectivity from multi-site spike signal recordings," *Neuroinformatics*, vol. 16, pp. 15–30, 2018.

[9] Oliver Faust, Yuki Hagiwara, Tan Jen Hong, Oh Shu Lih, and U Rajendra Acharya, "Deep learning for healthcare applications based on physiological signals: A review," *Computer methods and programs in biomedicine*, vol. 161, pp. 1–13, 2018.

[10] Parya Aghasafari, Pei-Chi Yang, Divya C Kernik, Kazuho Sakamoto, Yasunari Kanda, Junko Kurokawa, Igor Vorobyov, and Colleen E Clancy, "A deep learning algorithm to translate and classify cardiac electrophysiology," *Elife*, vol. 10, pp. e68335, 2021.

[11] Elif Izci, Mehmet Akif Ozdemir, Murside Degirmenci, and Aydin Akan, "Cardiac arrhythmia detection from 2d ecg images by using deep learning technique," in *2019 medical technologies congress (TIPTEKNO)*. IEEE, 2019, pp. 1–4.

[12] Charles A Ellis, Rongen Zhang, Darwin A Carbajal, Robyn L Miller, Vince D Calhoun, and May D Wang, "Explainable sleep stage classification with multimodal electrophysiology time-series," in *2021 43rd Annual International Conference of the IEEE Engineering in Medicine & Biology Society (EMBC)*. IEEE, 2021, pp. 2363–2366.

[13] Ijaz Ahmad, Xin Wang, Mingxing Zhu, Cheng Wang, Yao Pi, Javed Ali Khan, Siyab Khan, Oluwarotimi Williams Samuel, Shixiong Chen, and Guanglin Li, "Eeg-based epileptic seizure detection via machine/deep learning approaches: A systematic review," *Computational Intelligence and Neuroscience*, vol. 2022, 2022.

[14] Shu Lih Oh, Yuki Hagiwara, U Raghavendra, Rajamanickam Yuvaraj, N Arunkumar, M Murugappan, and U Rajendra Acharya, "A deep learning approach for parkinsons disease diagnosis from eeg signals," *Neural Computing and Applications*, vol. 32, pp. 10927–10933, 2020.

[15] Mohamed Hosny, Minwei Zhu, Wenpeng Gao, and Yili Fu, "A novel deep learning model for stn localization from lfps in parkinsons disease," *Biomedical Signal Processing and Control*, vol. 77, pp. 103830, 2022.

[16] Alessio P Buccino, Michael Kordovan, Torbjørn V Ness, Benjamin Merkt, Philipp D Häfliger, Marianne Fyhn, Gert Cauwenberghs, Stefan Rotter, and Gaute T Einevoll, "Combining biophysical modeling and deep learning for multielectrode array neuron localization and classification," *Journal of neurophysiology*, vol. 120, no. 3, pp. 1212–1232, 2018.

[17] Alessio P Buccino, Torbjørn V Ness, Gaute T Einevoll, Gert Cauwenberghs, and Philipp D Häfliger, "A deep learning approach for the classification of neuronal cell types," in *2018 40th Annual International Conference of the IEEE Engineering in Medicine and Biology Society (EMBC)*. IEEE, 2018, pp. 999–1002.

[18] Yuri Bozzi, Giovanni Provenzano, and Simona Casarosa, "Neurobiological bases of autism–epilepsy comorbidity: a focus on excitation/inhibition imbalance," *European Journal of Neuroscience*, vol. 47, no. 6, pp. 534–548, 2018.

[19] Carl E Stafstrom, "Recognizing seizures and epilepsy: insights from pathophysiology," *epilepsy*, pp. 1–9, 2014.

[20] Monica Frega, Sebastianus HC Van Gestel, Katrin Linda, Jori Van Der Raadt, Jason Keller, Jon-Ruben Van Rhijn, Dirk Schubert, Cornelis A Albers, and Nael Nadif Kasri, "Rapid neuronal differentiation of induced pluripotent stem cells for measuring network activity on micro-electrode arrays," *JoVE (Journal of Visualized Experiments)*, , no. 119, pp. e54900, 2017.

[21] Alessandro Maccione, Mauro Gandolfo, Paolo Massobrio, Antonio Novellino, Sergio Martinoia, and Michela Chiappalone, "A novel algorithm for precise identification of spikes in extracellularly recorded neuronal signals," *Journal of neuroscience methods*, vol. 177, no. 1, pp. 241–249, 2009.

[22] Paolo Didier Alfano, Vito Paolo Pastore, Lorenzo Rosasco, and Francesca Odone, "Fine-tuning or top-tuning? transfer learning with pretrained features and fast kernel methods," *arXiv e-prints*, pp. arXiv–2209, 2022.